

# THE GRAVITATIONAL COLLAPSE OF A UNIFORM SPHEROID

C. C. LIN, L. MESTEL,\* AND F. H. SHU†

Department of Mathematics, Massachusetts Institute of Technology

Received March 29, 1965

## ABSTRACT

A uniform, non-rotating, pressure-free spheroid is supposed to collapse gravitationally from rest. It is shown that the initial eccentricity is steadily increased by the anisotropic gravitational field: an initially oblate spheroid tends toward a disk, and an initially prolate spheroid toward a spindle. Numerical results are computed for a series of initial eccentricities.

## I. INTRODUCTION

In cosmogonical studies there arises naturally the problem of the collapse from rest of a cool, self-gravitating cloud. In the simplest idealization, with the cloud density initially spherically symmetric, the collapse clearly takes place through a series of spherically symmetric states, because of the isotropy of the gravitational field. A convenient Lagrangian coordinate is the radius  $r(m, t)$  at time  $t$  of the subsphere containing mass  $m$ . With pressure negligible, the equation of motion is

$$\frac{d^2 r}{dt^2} = -\frac{Gm}{r^2}; \quad (1)$$

this integrates to

$$r(m, t) = r_0(m) \cos^2 \theta, \quad (2)$$

where

$$\theta + \frac{1}{2} \sin 2\theta = t \left[ \frac{8\pi}{3} G \bar{\rho}_0(m) \right]^{1/2}, \quad (3)$$

and  $\bar{\rho}_0(m) = m/(4\pi r_0^3/3)$  is the mean density of the mass sphere,  $m$ , at the initial state of rest ( $t = 0$ ). If in particular the sphere has a uniform density  $\rho_0$  at  $t = 0$ , then  $\theta$  and so also  $r/r_0$  are functions of time only; a uniform sphere contracts homologously, and so stays uniform. The same result holds if at  $t = 0$  each shell is not at rest but is contracting with a speed proportional to  $r_0$ .

The instability of such a sphere against the formation of subcondensations—the “fragmentation” problem (Hoyle 1953)—is currently exciting much interest (Hunter 1962, 1964; Layzer 1963). In this paper, however, we are concerned with the more elementary question—the stability of the cloud as a whole against a change of shape that leaves the density uniform. It is shown that the state of spherical collapse is singular: the slightest over-all departure from sphericity is systematically magnified. The significance of this result will be discussed elsewhere (Mestel 1965): it is relevant to the asymptotic state achieved by a fragmenting cloud and to the contraction, with or without breakup, of a strongly magnetic cloud. In this paper, however, we shall assume that no breakup occurs, and ignore all forces other than gravitation.

## II. THE EQUATIONS TO THE PROBLEM

Although the detailed calculations below are performed just for axially symmetric bodies, the basic result is valid for all uniform ellipsoids and is most easily established in

\* Department of Applied Mathematics and Theoretical Physics, University of Cambridge, Cambridge, England.

† Now at Department of Astronomy, Harvard University.

symmetric notation. In a study of the flattening of a *uniformly rotating* uniform sphere, Lynden-Bell (1962, 1964) pointed out that collapse from an initial state of pure rotation will be through a series of uniform spheroids of steadily increasing eccentricity. The essence of the proof depends on the gravitational potential within a uniform spheroid being quadratic in Cartesian coordinates, and it is immediately applicable to the present problem with zero rotation, but with the initial anisotropy due not to centrifugal force but to an anisotropic mass distribution.

For collapse to occur through a series of uniform ellipsoids, a particle with coordinates  $(x_0, y_0, z_0)$  at time  $t = 0$  must subsequently be at  $(x, y, z)$  with

$$x = x_0 X(t), \quad y = y_0 Y(t), \quad z = z_0 Z(t); \quad (4)$$

i.e.,  $X$ ,  $Y$ , and  $Z$  must be independent of  $(x_0, y_0, z_0)$ , so that  $x$ ,  $y$ , and  $z$  are individually subjected to *homologous* transformations that maintain both the ellipsoidal shape and a uniform density

$$\rho = \frac{\rho_0}{X Y Z} \quad (5)$$

but alter the ratios of axes (except in the degenerate case  $X = Y = Z$ ). The potential inside a uniform ellipsoid is (Lyttleton 1953)

$$V = -\pi G \rho (a x^2 + \beta y^2 + \gamma z^2 - \delta), \quad (6)$$

where

$$a = a b c \int_0^\infty \frac{d\lambda}{(a^2 + \lambda)\Delta} \text{ etc.}, \quad \delta = a b c \int_0^\infty \frac{d\lambda}{\Delta}, \quad (7)$$

and

$$\Delta^2 = (a^2 + \lambda)(b^2 + \lambda)(c^2 + \lambda). \quad (8)$$

The quantities  $a$ ,  $\beta$ , and  $\gamma$  depend only on the ratios  $a:b:c$ . Thus, the equations of motion of a point mass at  $(x, y, z)$

$$\frac{d^2 x}{dt^2} = -2\pi G \rho a x, \quad \frac{d^2 y}{dt^2} = -2\pi G \rho \beta y, \quad \frac{d^2 z}{dt^2} = -2\pi G \rho \gamma z \quad (9)$$

reduce, by the relations (4) and (5), to

$$\frac{d^2 X}{dt^2} = -\left(\frac{2\pi G \rho_0}{X Y Z}\right) a X, \quad (10)$$

etc. At  $t = 0$ ,

$$X = Y = Z = 1, \quad \frac{dX}{dt} = \frac{dY}{dt} = \frac{dZ}{dt} = 0. \quad (11)$$

Thus, since both equation (10) and initial conditions (11) are independent of  $(x_0, y_0, z_0)$ , so are also the functions  $X(t)$ ,  $Y(t)$  and  $Z(t)$ , and the collapse is through a series of uniform ellipsoids. The same result clearly holds under the relaxed condition with  $dX/dt$ ,  $dY/dt$ ,  $dZ/dt$  initially not zero but merely independent of  $(x_0, y_0, z_0)$ . Further, if, for definiteness,

$$a > b > c, \quad (12)$$

then by equations (7)

$$a < \beta < \gamma, \quad (13)$$

and from equations (10)

$$-\frac{1}{X} \frac{d^2 X}{dt^2} < -\frac{1}{Y} \frac{d^2 Y}{dt^2} < -\frac{1}{Z} \frac{d^2 Z}{dt^2} \quad (14)$$

the ratios  $a:b:c$  steadily increase with time, when the initial conditions  $dX/dt = dY/dt = dZ/dt = 0$  are imposed. In particular, an oblate spheroid increases in eccentricity and approaches an infinitely thin disk (provided pressure can always be neglected); equally, a prolate spheroid becomes an infinitely thin cylinder.

### III. SOLUTION OF THE EQUATIONS

For computation of the spheroidal cases, we use cylindrical coordinates  $(\varpi, \phi, z)$ , which are related to initial values  $(\varpi_0, \phi_0, z_0)$  by

$$\varpi = \varpi_0 R(t), \quad z = z_0 Z(t), \quad \phi = \phi_0. \quad (15)$$

The potential (6) can be written

$$V = \text{constant} - \frac{G\rho}{2} [A(e)\varpi^2 + C(e)z^2], \quad (16)$$

where  $A$  and  $C$  are known functions of the instantaneous eccentricity  $e$ . The analogues of equation (10) are

$$\frac{d^2R}{dt^2} = -\frac{G\rho_0 A(e)}{RZ} \quad (17)$$

and

$$\frac{d^2Z}{dt^2} = -\frac{G\rho_0 C(e)}{R^2} \quad (18)$$

with

$$Z^2 = R^2 \frac{(1+e^2)}{(1-e^2)} \quad (19a)$$

for an oblate spheroid, and

$$R^2 = Z^2 \frac{(1-e^2)}{(1-e_0^2)} \quad (19b)$$

for a prolate spheroid. Equations (17) and (18) must be solved subject to the initial condition at  $t = 0$ :

$$R = Z = 1, \quad dR/dt = dZ/dt = 0. \quad (20)$$

For the oblate case

$$A(e) = \frac{2\pi(1-e^2)}{e^3} [\sin^{-1} e - e(1-e^2)^{1/2}], \quad (21)$$

$$C(e) = \frac{4\pi}{e^2} \left[ 1 - \frac{(1-e^2)^{1/2}}{e} \sin^{-1} e \right]; \quad (22)$$

for the prolate case

$$A(e) = \frac{2\pi}{e^2} \left[ 1 - \frac{1-e^2}{2e} \log \frac{(1+e)}{(1-e)} \right], \quad (23)$$

$$C(e) = \frac{4\pi(1-e^2)}{e^2} \left[ -1 + \frac{1}{2e} \log \frac{(1+e)}{(1-e)} \right] \quad (24)$$

(McMillan 1958).

#### a) Solution for the Case of Oblate Spheroids

To fix our ideas, let us first consider the case of the oblate spheroid. In this case, the equations to be integrated are (17) and (18), with  $A(e)$  and  $C(e)$  defined by equations

(21) and (22), and  $e$  defined by equation (19a). The initial conditions are given by (20).

In order to get analytical solutions, we adopt variables suggested by the spherical case, in which

$$R = Z, \quad e = 0, \quad A(e) = C(e) = 4\pi/3, \quad (25a)$$

and the solution is given by

$$R = \cos^2 \theta, \quad V = -(8\pi/3)^{1/2} \tan \theta, \quad \tau = (8\pi/3)^{-1/2} (\theta + \frac{1}{2} \sin 2\theta) \quad (25b)$$

where

$$\tau \equiv (G\rho_0)^{1/2} t, \quad V \equiv dR/d\tau. \quad (26)$$

Thus, for oblate spheroids, we use the same definitions (26) and introduce  $\theta$  and  $x$  by

$$R = \cos^2 \theta, \quad x = \tan \theta \quad (27)$$

as the more convenient variables. We also introduce a parameter  $a$  through the relation

$$V = \frac{dR}{d\tau} = -a \tan \theta. \quad (28)$$

We further define  $E$ ,  $\psi$ , and  $Q$  by (cf. eq. [19a])

$$E = \frac{Z}{R} = \frac{(1 - e^2)^{1/2}}{(1 - e_0^2)^{1/2}} = \frac{\cos \psi}{\cos \psi_0}, \quad (29a)$$

$$Q = R^2 \frac{dE}{d\tau}. \quad (29b)$$

The system of equations to be integrated then becomes

$$x \frac{d\alpha^2}{dx} + 2\alpha^2 = \frac{4A}{E}, \quad (30)$$

$$\frac{dE}{dx} = \frac{2Q}{a}, \quad (31)$$

$$(1 + x^2) \frac{dQ}{dx} = \frac{2(A - C)}{a}, \quad (32)$$

where  $E$  is given by equation (29a), and

$$A = 2\pi - \frac{C}{2}, \quad (33a)$$

$$C = 4\pi (\sin \psi)^{-3} (\sin \psi - \psi \cos \psi). \quad (33b)$$

Note that in the spherical case ( $A = C = 4\pi/3$ ), the variables to be sought in equations (30)–(32) are all constants:

$$Q = 0, \quad E = 1, \quad \text{and} \quad \alpha^2 = \frac{2A}{E} = \frac{8\pi}{3}. \quad (34)$$

The solution then takes on the form (25) given above.

Corresponding to equation (20), equations (30)–(32) are to be integrated under the following initial conditions at  $x = 0$ :

$$\alpha = \alpha_0 = (2A_0)^{1/2}, \quad E = E_0 = 1, \quad Q = 0, \quad (35)$$

where  $A_0$  and  $E_0$  are the values of  $A$  and  $E$  evaluated at  $\psi = \psi_0$  according to equations (29) and (33). The initial eccentricity  $e_0$  remains a parameter of the problem.

We shall attempt to express the solutions in powers of  $x$ . If this does not carry the solution far enough in any particular case, the numerical method<sup>1</sup> will be used to give more accurate results. It actually turns out that two or three terms of the series solution give extremely accurate answers right up to the collapse of the oblate spheroids into a disk, if the spheroid has a fair amount of initial oblateness. Even when the initial flattening is as little as 10 per cent (minor axis:major axis = 0.90), the results are moderately accurate. In this case, the time of collapse obtained by the series solution is 0.536 (when the series is used up to three terms for  $A$ ,  $C$ , and  $E$ ) while numerical integration gives 0.538. The ratio “collapse radius”: “initial radius” is 0.140 by series method and 0.134 by numerical integration. (For further details, see Table 1 and Fig. 1.)

TABLE 1\*  
NUMERICAL VALUES AT COLLAPSE FOR NATURAL  
TIME AND RADIUS FOR OBLATE CASE

$z_0/\omega_0$	$e_0$	$\tau_c$ (Series Solution)	$\tau_c$ (Numerical Integration)	$\omega_c/\omega_0$ (Series Solution)	$\omega_c/\omega_0$ (Numerical Integration)
0 95	0 312	0 539	0 541	0 0868	0 0744
90	436	536	538	140	134
80	600	527	529	252	251
70	714	516	518	358	360
60	800	504	505	461	464
50	866	489	492	560	563
40	917	474	477	655	658
30	954	457	462	747	750
20	980	439	447	835	838
0 10	0 995	0 419	0 428	0 920	0 917

\* Here  $\tau_c$  is the dimensionless time (eq [26]) at which collapse into a disk occurs. The parameter  $e_0$  denotes the initial eccentricity of the spheroid and  $Z_0/\omega_0$  denotes the ratio of its minor axis to radius (major axis). The ratio  $\omega_c/\omega_0$  is the disk radius as a fraction of that of the initial spheroid.

The power series for the various quantities are calculated as follows. First, we note that the initial conditions require that  $\alpha$ ,  $A$ ,  $C$ ,  $E$  are all even in  $x$ , and that  $Q$  is odd in  $x$ , when they are calculated from equations (30)–(32). Thus, we may write

$$\alpha = \alpha_0 + \alpha_2x^2 + \alpha_4x^4 + \dots, \quad (36)$$

$$A = A_0 + A_2x^2 + A_4x^4 + \dots, \quad (37)$$

$$C = C_0 + C_2x^2 + C_4x^4 + \dots, \quad (38)$$

$$E = E_0 + E_2x^2 + E_4x^4 + \dots, \quad (E_0 = 1) \quad (39)$$

$$Q = Q_1x + Q_3x^3 + \dots \quad (40)$$

<sup>1</sup> Kutta-Runge procedure, as extended by Gill (1953)

Note that the variables  $A$ ,  $C$ , and  $E$  must be related to each other, since they are all defined in terms of  $\psi$  (see eqs. [29] and [33]). By introducing these relations and by making use of equations (30)–(32), the coefficients can all be determined in terms of the initial eccentricity  $e_0$ . The details of these calculations are given in Appendix I. The more important coefficients are given explicitly in equations (A5a)–(A5e).

After the series (36) and (39) are calculated, we can easily integrate equation (28) for the time  $\tau$  in terms of  $x = \tan \theta$ . We obtain

$$\alpha_0 \tau = \left( \theta + \frac{1}{2} \sin 2\theta \right) - \frac{\alpha_2}{\alpha_0} \left( \theta - \frac{1}{2} \sin 2\theta \right). \tag{41}$$

In this form, it is apparent that, when  $\alpha_2/\alpha_0$  and  $\theta$  are moderately small, the change in  $\tau(\theta)$  is given essentially by the scale factor  $\alpha_0$ .

*Numerical results.*—The quantity  $E = Z/R$  is expressed in terms of  $\theta$  via equation (39), where  $x = \tan \theta$  according to definition (27). The dimensionless time  $\tau = (G\rho_0)^{+1/2} t$

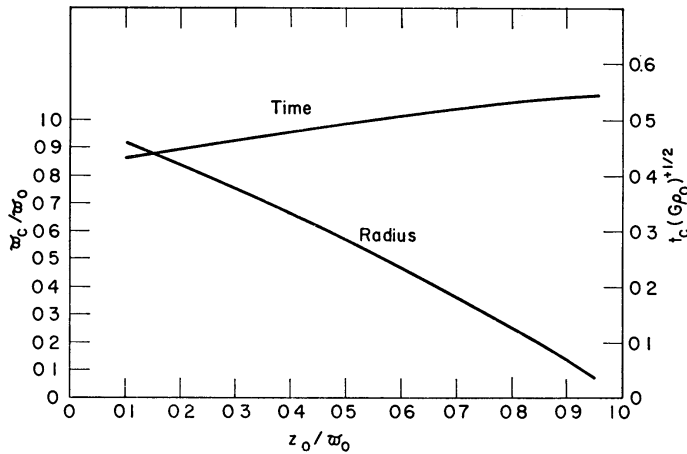


FIG. 1.—“Collapse” values for oblate spheroids as computed by numerical integration. The abscissa is the initial ratio of the minor axis to the major axis. The radius of the final disk as a fraction of the initial radius of the oblate spheroid is shown by the curve marked “radius,” with vertical scale marked on the left. The “natural” time  $\tau_c = t_c(G\rho_0)^{+1/2}$  at collapse into a disk is shown by the curve marked “time,” with vertical scale marked on the right. Corresponding plots of the collapse values as given by series solution would be virtually indistinguishable from the ones given here.

is also expressed in terms of  $\theta$  by expression (41). Thus, equations (27), (39), and (41) give the parametric representation of  $Z(\tau)$  and  $R(\tau)$ . Only the terms that appear explicitly in these equations are needed for sufficient accuracy. All of the coefficients needed can be determined in terms of the initial eccentricity  $e_0$  by means of equation (A5) in Appendix I.

Two quantities of general interest are (a) the time required for complete collapse of the spheroid into a disk, and (b) the radius of this disk as a fraction of the initial radius of the spheroid. These are given in Table 1.

Corresponding results for these “collapse values” were also obtained by numerical integration, and they are shown for comparison. These were obtained by the Kutta-Runge method with  $z(M,t)/\varpi(M,t) = E(t) \cos \psi_0$  as the independent variable, where  $\varpi(M,t)$  is the radius of the entire spheroid of mass  $M$  at time  $t$  and  $z(M,t)$  is the semi-minor axis. It was found necessary to start the calculation by using the series solution for a small initial interval (e.g., from  $E \cos \psi_0 = 0.95$  to  $0.94$ ). The machine calculation was then carried out to  $E \cos \psi_0 = 0.01$ , and the “collapse values” themselves were obtained

by extrapolation. It is seen that the agreement is close between results obtained by the two methods. These results are also shown in Figure 1.

The history of the collapse is shown in Figure 2. Almost identical results are obtained by series solution and by numerical integration.

*b) Solution for the Case of Prolate Spheroids*

Although the following discussion for the prolate case will be found to be very similar to that in the previous section, it is thought desirable to give a complete treatment, precisely because a cross-reference would cause endless confusion. In this case, the equations to be integrated are equations (17) and (18), with  $A(e)$  and  $C(e)$  given by equations (23)

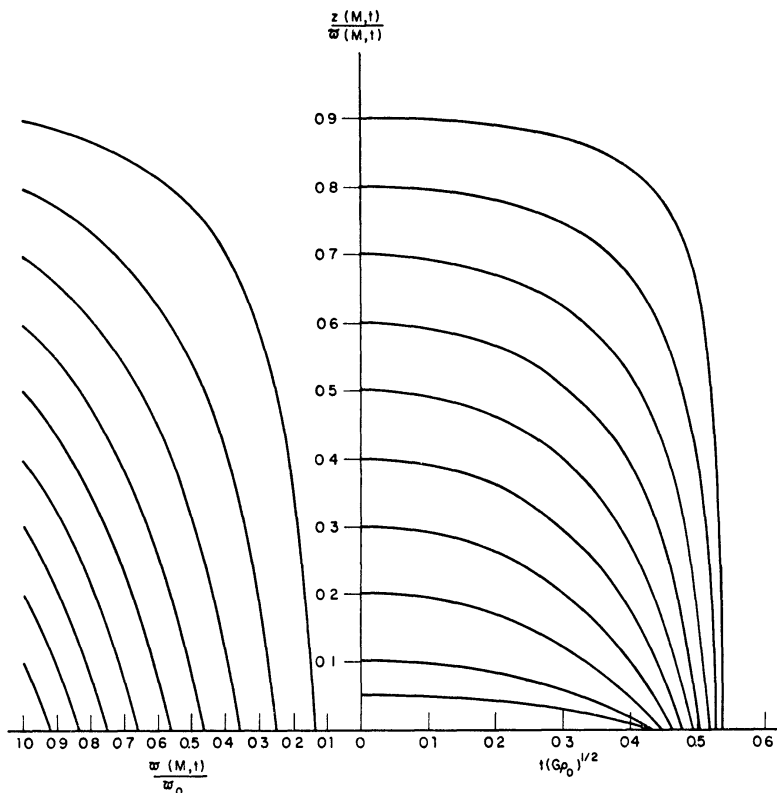


FIG. 2.—History of collapse of oblate spheroids as computed by numerical integration. The ordinate is the instantaneous ratio of the minor axis to the major axis. The abscissa running to the right is the “natural” time  $\tau = t(G\rho_0)^{+1/2}$  and the abscissa running to the left is the instantaneous radius as a fraction of the initial radius of the oblate spheroids. Curves are shown for various values of initial oblateness (which may be read off the vertical axis for the initial conditions  $t = 0, w/w_0 = 1$ ). Corresponding plots of the history of collapse as given by series solution would be virtually indistinguishable from the ones given here.

and (24), and  $e$  defined by equation (19b). The initial conditions are given by equation (20).

In analogy with the oblate case, we define  $\theta$  and  $x$  by

$$Z = \cos^2 \theta, \quad x = \tan \theta \tag{42}$$

and define  $W$  and  $a$  through

$$W = \frac{dZ}{d\tau} = -a \tan \theta, \tag{43}$$



where  $\tau \equiv (G\rho_0)^{+1/2} t$ . We further define  $E$  by

$$E \equiv \frac{R}{Z} = \frac{(1 - e^2)^{1/2}}{(1 - e_0^2)^{1/2}}. \quad (44)$$

Note that although  $E$  in equation (44) stands in the same relation to  $e$  as it does in equation (29), its relation to the semimajor axis and the radius is reversed.

By introducing the variable

$$Q \equiv Z^2 \frac{dE}{d\tau}, \quad (45)$$

the system of equations to be integrated becomes

$$x \frac{d\alpha^2}{dx} + 2\alpha^2 = \frac{4C}{E^2}, \quad (46)$$

$$\frac{dE}{dx} = \frac{2Q}{a}, \quad (47)$$

$$(1 + x^2) \frac{dQ}{dx} = \frac{2(C - A)}{aE}, \quad (48)$$

where  $E$  is given by expression (44) and

$$A = 2\pi - \frac{C}{2}, \quad (49a)$$

$$C = 4\pi \frac{1 - e^2}{e^2} \left( -1 + \frac{1}{2e} \log \left| \frac{1 + e}{1 - e} \right| \right). \quad (49b)$$

Corresponding to equation (20), equations (46)–(48) are to be integrated under the initial conditions

$$a = a_0 = (2C_0)^{1/2}, \quad E = E_0 = 1, \quad Q = 0 \quad (50)$$

at  $x = 0$ , where  $C_0$  and  $E_0$  are the values of  $C$  and  $E$  evaluated at  $e = e_0$ . The initial eccentricity  $e_0$  remains a parameter of the problem.

Upon comparison with the oblate case, we notice that all equations (42)–(48) can be obtained from their oblate case counterparts through the formal transformation

$$\text{Oblate} \rightarrow \text{Prolate}, \quad R \rightarrow Z, \quad Z \rightarrow R, \quad V \rightarrow W, \quad A \rightarrow C/E, \quad C \rightarrow A/E. \quad (51)$$

The last two transformations lead to the slight disparity between the formal results obtained for the prolate case and the oblate case. These differences arise from the fact that the original equations of motion (17) and (18) are themselves unsymmetrical in  $R$  and  $Z$ .

A power series solution in  $x$  may be developed with  $a$ ,  $A$ ,  $C$ , and  $E$  all even in  $x$  and  $Q$  odd in  $x$  as required by initial condition (50). Thus, we have

$$a = a_0 + a_2x^2 + a_4x^4 + \dots, \quad (52)$$

$$A = A_0 + A_2x^2 + A_4x^4 + \dots, \quad (53)$$

$$C = C_0 + C_2x^2 + C_4x^4 + \dots, \quad (54)$$

$$E = E_0 + E_2x^2 + E_4x^4 + \dots, \quad (55)$$

$$Q = Q_1x + Q_3x^3 + \dots \quad (56)$$



The set of equations (44), (46), (47), (48), and (49) forms a complete set for the determination of the coefficients in equations (52)–(56) in terms of the initial eccentricity  $e_0$ . The details of this calculation are given in Appendix II.

The recovery of time is effected in the analogous way to the oblate case by integration of equation (43), and leads to the same formal relation (41). The coefficients  $a_0, a_2, \dots$ , of course, depend on the initial eccentricity  $e_0$  in a manner different from that in the oblate case.

*Numerical results.*—It turns out that the series solutions for prolate spheroids are somewhat less accurate than their oblate counterparts. The convergence is less rapid because the ratios of successive coefficients in the expansions for  $E$ ,  $a$ , and  $Q$  in powers of  $x$  are larger in the prolate case for the same initial eccentricity. This difference is accentuated for larger initial eccentricities. An indication of this behavior is seen upon comparison of the values of the important ratios  $E_4/E_2$  and  $a_2/a_0$  for the prolate and oblate cases at initial eccentricity  $e_0 = 1$  (cf. Tables A1 and A2).

TABLE 2\*  
NUMERICAL VALUES AT COLLAPSE FOR NATURAL TIME AND  
SEMIMAJOR AXIS FOR PROLATE CASE

$\omega_0/z_0$	$e_0$	$\tau_c$ (Series Solution)	$\tau_c$ (Numerical Integration)	$Z_c/Z_0$ (Series Solution)	$Z_c/Z_0$ (Numerical Integration)
0 95	0 312	0 527	0 542	0 200	0 0842
90	436	523	541	263	150
80	600	518	539	368	276
70	714	514	536	464	397
60	800	511	532	558	511
50	866	508	529	649	620
40	917	505	526	739	722
30	954	502	524	824	816
20	980	500	523	902	900
0 10	0 995	0 498	0 521	0 966	0 966

\* Notation here similar to that in Table 1

Nevertheless, the series results for the collapse values do not suffer badly upon comparison with those obtained by numerical integration, provided the prolate spheroid is initially sufficiently elongated. Thus, when the initial elongation is 30 per cent (minor axis:major axis = 0.70), the time of collapse obtained by the series solution is 0.514 as compared to the value 0.536 by numerical integration; the ratio “collapse major axis”: “initial major axis” is 0.464 by series solution and 0.397 by numerical integration. Other collapse values for different initial eccentricities are given in Table 2, and are shown graphically in Figure 3.

The numerical integration uses a four-step Runge-Kutta method (see Gill 1953) with  $\omega/z = (1 - e_0^2)^{1/2} E$  as the independent variable. The same procedure used before is followed in starting the integration process with the help of the series solution, and in terminating it before “collapse.”

The history of the collapse obtained by series solution and by numerical integration is shown in Figure 4. The agreement between the two calculations in the initial stages justifies the use of the series solution itself to start the numerical integration.

#### IV. DISCUSSION

It must be emphasized that the systematic increase in eccentricity is a purely gravitational effect: it is due not to a force that is essentially anisotropic (such as centrifugal force) but to the gravitational field of a non-isotropic distribution of sources. The effect

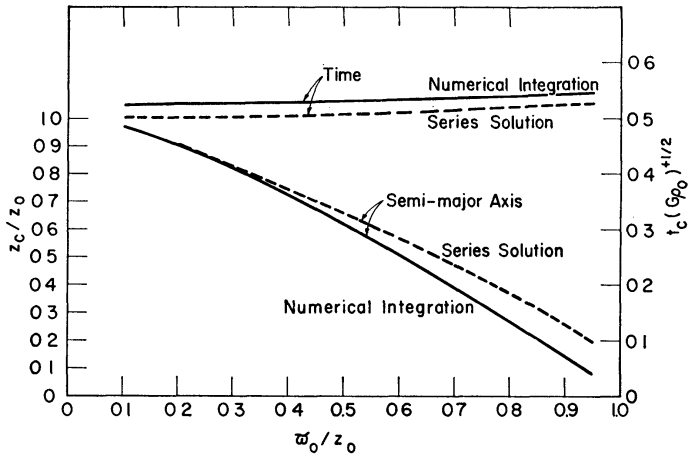


FIG. 3.—“Collapse” values for prolate spheroids. The abscissa is the initial ratio of the minor axis to the major axis. The major axis of the final spindle as a fraction of the initial major axis of the prolate spheroid is shown by the curve marked “semimajor axis,” with vertical scale marked on the left. The “natural” time  $\tau_c = t_c(G\rho_0)^{1/2}$  at collapse into a disk is shown by the curve marked “time,” with vertical scale marked on the right. Values as computed by numerical integration are shown in solid lines; those computed by series solution are shown in dotted lines.

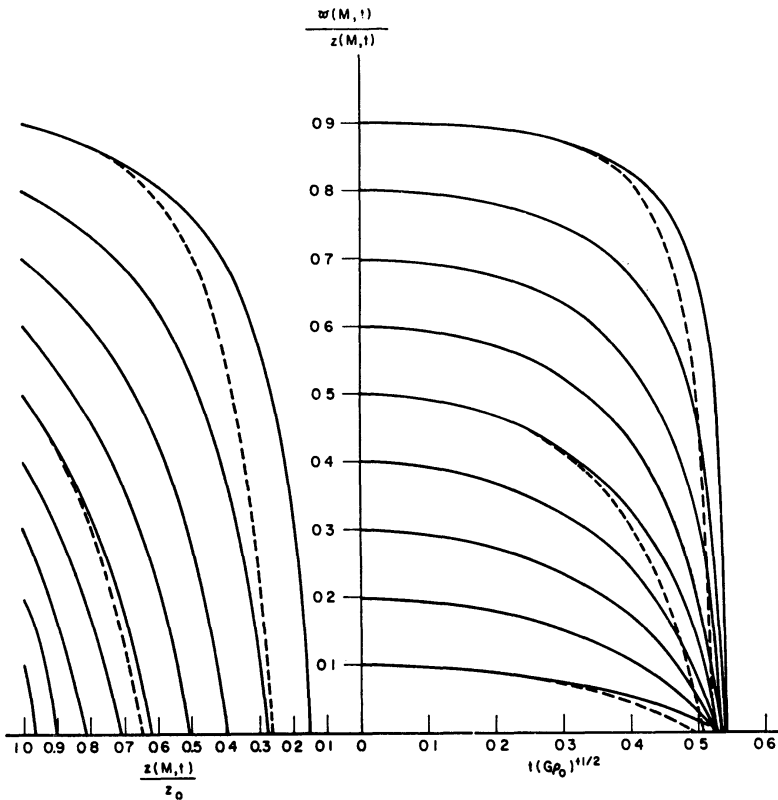


FIG. 4.—History of collapse of prolate spheroids. The ordinate is the instantaneous ratio of the minor axis to the major axis. The abscissa running to the right is the “natural” time  $\tau$ , and the abscissa running to the left is the instantaneous major axis as a fraction of the initial major axis of the prolate spheroids. Curves are shown for various values of initial prolateness (which may be read off the vertical axis for the initial conditions  $t = 0, \omega/\omega_0 = 1$ ). Those in solid lines are computed by numerical integration. Three cases of varying initial prolateness ( $\omega_0/z_0 = 0.9, 0.5,$  and  $0.1$ ) as computed by series solution are plotted in dotted lines and offered for comparison. The left curves for  $\omega_0/z_0 = 0.1$  as computed by series solution and numerical integration are virtually indistinguishable throughout the collapse process.

would not occur in a star, which by definition is a body maintained very close to hydrostatic equilibrium, with the isotropic thermal pressure the main force opposing gravity: a slight oblateness in a non-rotating star, for example, would be reversed by the excess pressure gradient along the axis of oblateness, and the star would execute non-radial oscillations.

The assumption of zero pressure gradients is only an approximation. Even in a uniform gas cloud, the density gradient is large at the edge, and there will be an isothermal pressure gradient that is locally large. A more realistic model would have a density that is nearly uniform over the bulk of the cloud, but decreases monotonically toward the edge. If the cloud is strictly spherical and contracts from an initial state with negligible pressure gradients, then since  $d\bar{\rho}/dm < 0$ , solution (3) shows that the outer shells lag behind the inner ones, and the isothermal pressure gradient becomes a still smaller fraction of the gravitational force density. However, if the cloud is initially oblate, then once it has become highly flattened, with a semithickness  $\bar{z}$ , the ratio of the  $z$ -pressure gradient to the  $z$ -component of gravity is  $(c^2/\lambda)/4\pi G\rho\bar{z}$ , where  $\lambda$  is a density scale height,  $c$  is the isothermal sound speed, and the value  $4\pi$  has been taken from the limit of equation (22) as  $\epsilon \rightarrow 1$ . Thus, since  $\rho\bar{z}$  stays constant by mass conservation, an isothermal pressure is able to halt indefinite flattening, and the spheroid will oscillate. When the kinetic energy of the oscillation has all been dissipated and radiated away, the cloud (still assumed unfragmented) will achieve hydrostatic  $z$ -equilibrium, with a semithickness  $\bar{z}$  given by

$$\bar{z} \cong \left( \frac{c^2}{2\pi G\rho} \right)^{1/2} \quad (57)$$

(Spitzer 1942; Ledoux 1951). The  $\varpi$ -component of gravity will be effectively unopposed, and free fall will continue in two dimensions, with  $\bar{z}$  adjusting itself so as to satisfy (57) approximately. If  $\bar{\omega}$  is the instantaneous equatorial radius, then the cloud mass  $M \cong 4\pi\rho\bar{z}\bar{\omega}^2/3$ , and

$$\frac{\bar{z}}{\bar{\omega}} \cong \frac{M c^2}{3GM^2/2\bar{\omega}} \propto \bar{\omega}. \quad (58)$$

Thus the oblateness continues to increase, though at a rate determined by free fall in the  $\varpi$ -direction only.

If, however, the cloud is initially prolate, then once it has become quasi-cylindrical, the ratio of pressure to gravitational force becomes (by eq. [23])  $\cong (c^2/\lambda)/2\pi G\rho\bar{\omega}$ , which behaves like  $\bar{\omega}/\lambda$ , since in cylindrical motion  $\rho \propto \bar{\omega}^{-2}$ . Thus an initially weak isothermal pressure gradient stays weak during isothermal cylindrical collapse (McCrea 1957): indefinite collapse will be halted only by departure from adiabatic process or by non-thermal forces such as magnetic force (Chandrasekhar and Fermi 1953; Mestel 1965; Strittmatter 1965).

## APPENDICES

### I. DETERMINATION OF THE COEFFICIENTS IN EQUATIONS (36)–(40)

The most important quantities to be calculated are  $E$  and  $\alpha$ . When equations (36)–(40) are substituted into equations (30)–(32), we obtain (noting that  $E_0 = 1$ )

$$E_2 = 1 - C_0/A_0, \quad (A1)$$

$$E_4 = (6A_0^2)^{-1}[A_2C_0 - A_0C_2 - C_0(A_0 - C_0)], \dots, \quad (A2)$$

and

$$\alpha_0 = (2A_0)^{1/2}, \quad (A3)$$

$$\frac{\alpha_2}{\alpha_0} = (4A_0)^{-1}(A_2E_0 - A_0E_2). \quad (A4)$$

The above relations are insufficient for determining all the coefficients until the relationships among the coefficients for  $A$ ,  $C$ , and  $E$  are introduced. This step is carried out below. The results for some of the more important coefficients are as follows:

$$E_0 = 1, \quad E_2 = 3 - 4\pi/a_0, \tag{A5a}$$

$$E_4/E_2 = \frac{1}{3}(\chi - \sin \chi)^{-2}[\chi^2 + \chi \sin \chi - 4(1 - \cos \chi)], \tag{A5b}$$

$$a_0 = (2a_0)^{1/2}, \quad \frac{a_2}{a_0} = \frac{E_2^2}{4} \frac{1 + \cos \chi}{1 - \cos \chi}, \tag{A5c}$$

TABLE A1  
NUMERICAL VALUES FOR CERTAIN IMPORTANT  
COEFFICIENTS IN OBLATE CASE

$\psi_0$	$a_0$	$a_2/a_0$	$E_2$	$E_1/E_2$
0	2 895	0	0	0 0333
$\pi/4$	2 678	0 0635	-0 504	039
$\pi/3$	2 437	126	-1 230	043
$5\pi/12$	1 955	245	-3 58	052
$\pi/2$	0	0 405	$-\infty$	0 0632

TABLE A1—Continued

$Z_0/\omega_0$	$E_2$	$E_2/E_2$	$a_0$	$a_2/a_0$	$Q_1$	$Q_3/Q_1$
1 00	0	0 0333	2 895	0	0	0 0667
0 95	- 0 0682	0375	2 86	0 00986	- 0 195	0849
0 90	- 0 134	0351	2 83	0191	- 0 379	0894
0 80	- 0 303	0371	2 76	0407	- 0 835	115
0 70	- 0 522	0392	2 67	0653	- 1 39	144
0 60	- 0 816	0416	2 57	0935	- 2 09	177
0 50	- 1 23	0442	2 44	126	- 3 00	215
0 40	- 1 86	0472	2 27	164	- 4 22	258
0 30	- 2 91	0505	2 06	209	- 5 99	310
0 20	- 5 02	0542	1 77	262	- 8 88	370
0 10	-11 4	0583	1 32	326	-15 0	443
0 05	-24 1	0607	0 963	364	-23 2	485
0 00	$-\infty$	0 0632	0	0 405	$-\infty$	0 531

where

$$a_0 = 2\pi \sin \chi(\chi - \sin \chi)/(1 - \cos \chi)^2, \tag{A5d}$$

and

$$\chi = 2\psi_0 = 2 \sin^{-1} e_0. \tag{A5e}$$

Numerical values for these coefficients are given in Table A1.

The final formulae used for the numerical calculations are as follows:

$$E = 1 + E_2(\tan \theta)^2 + E_4(\tan \theta)^4, \tag{A6a}$$

$$a_0\tau = (\theta + \frac{1}{2} \sin 2\theta) - (a_2/a_0)(\theta - \frac{1}{2} \sin 2\theta), \tag{A6b}$$

$$R = \cos^2 \theta, \tag{A6c}$$

and

$$Z = ER. \quad (\text{A6d})$$

*Expansion in Powers of  $\psi - \psi_0$*

To relate  $A$ ,  $C$ , and  $E$ , we expand them in powers of

$$\delta = \psi - \psi_0. \quad (\text{A7})$$

We have

$$A = a_0 + a_1\delta + a_2\delta^2 + \dots, \quad (\text{A8a})$$

$$C = c_0 + c_1\delta + c_2\delta^2 + \dots, \quad (\text{A8b})$$

$$E = \epsilon_0 + \epsilon_1\delta + \epsilon_2\delta^2 + \dots; \quad (\text{A8c})$$

and (since  $\delta$  is even in  $x$  and vanishes at  $x = 0$ )

$$\delta = \delta_2x^2 + \delta_4x^4 + \dots \quad (\text{A9})$$

The coefficients in the above expansions for  $A$ ,  $C$ , and  $E$  are obviously functions of  $\psi_0 = \sin^{-1} e_0$  only. The coefficients  $\delta_2, \delta_4, \dots$ , have to be determined from the differential equations, or alternatively, from the formulae (A1)–(A4).

Clearly, by comparing equations (37), (38), (39), and (A8), we have

$$A_0 = a_0, \quad C_0 = c_0, \quad E_0 = \epsilon_0 = 1. \quad (\text{A10})$$

By substituting equation (A9) into equations (A8), we get, by comparison with equations (37)–(39),

$$a_1\delta_2 = A_2, \quad a_1\delta_4 + a_2\delta_2^2 = A_4, \dots, \quad (\text{A11a})$$

$$c_1\delta_2 = C_2, \quad c_1\delta_4 + c_2\delta_2^2 = C_4, \dots, \quad (\text{A11b})$$

$$\epsilon_1\delta_2 = E_2, \quad \epsilon_1\delta_4 + \epsilon_2\delta_2^2 = E_4, \dots \quad (\text{A11c})$$

The successive coefficients in equations (A1)–(A4) can then be calculated explicitly by using them in alternate steps with equations (A11). Thus,  $E_2$  is determined from equation (13), which in turn defines  $\delta_2$  from equation (A11c);  $A_2, C_2$  are then obtained from equations (A11a) and (A11b), enabling  $E_4$  to be calculated. The results are as follows:

$$E_2 = 1 - c_0/a_0 \quad (\text{A12a})$$

$$E_4 = (6a_0^2\epsilon_1)^{-1} (a_1c_0 - a_0c_1 - a_0b_0\epsilon_1), \dots; \quad (\text{A12b})$$

$$a_0 = (2a_0)^{1/2} \quad (\text{A13a})$$

$$a_2/a_0 = (4a_0^2\epsilon_1)^{-1} (a_1 - a_0\epsilon_1)(a_0 - c_0) \dots \quad (\text{A13b})$$

[Note that since  $A + C/2 = 2\pi$ , we can also write  $E_4$  as

$$E_4/E_2 = (6a_0^2\epsilon_1)^{-1} (1 - 2\pi c_1 - a_0c_0\epsilon_1). \quad (\text{A12b}')] ]$$

The coefficients  $a_0, a_1, \dots, c_0, c_1, \dots, \epsilon_0, \epsilon_1, \dots$ , are as follows:

$$a_0 = 2\pi - \frac{c_0}{2}, \quad c_0 = 4\pi (\sin \psi_0)^{-3} (\sin \psi_0 - \psi_0 \cos \psi_0), \quad (\text{A14a})$$

$$a_1 = -\frac{c_1}{2}, \quad c_1 = 4\pi (\sin \psi_0)^{-3} \left[ \frac{\psi_0}{\sin \psi_0} (\sin^2 \psi_0 + 3 \cos^2 \psi_0) - 3 \cos \psi_0 \right] \quad (\text{A14b})$$

$$a_2 = -\frac{c_2}{2}, \quad (\text{A14c})$$

$$c_2 = 4\pi (\sin \psi_0)^{-3} [6 \cot^2 \psi_0 (\sin \psi_0 - \psi_0 \cos \psi_0) + 2 \sin \psi_0 - 4\psi_0 \cos \psi_0], \quad \dots, \quad (\text{A14d})$$

$$a_n = -\frac{c_n}{2}, \quad (\text{A14d})$$

$$\epsilon_0 = 1, \quad \epsilon_1 = -\tan \psi_0, \quad \epsilon_2 = -\frac{1}{2}, \dots \quad (\text{A14e})$$

By substituting these explicit expressions into equations (A12) and (A13), we get finally equations (A5).

## II. DETERMINATION OF THE COEFFICIENTS IN EQUATIONS (52)–(56)

We may obtain the coefficients in power series expansion in  $x$  of  $a$ ,  $E$ , and  $Q$  in terms of those of  $A$  and  $C$  either by direct substitution of equations (52)–(56) into the differential equations (46)–(48), or by comparison with the results of the oblate case with the help of the substitution rules given by equation (51). Both methods yield the same results, of course, and the corresponding relations to equations (A1)–(A4) are

$$E_0 = 1, \quad (\text{A15a})$$

$$E_2 = 1 - A_0/C_0, \quad (\text{A15b})$$

$$E_4 = (6C_0)^{-1} [A_0C_2 - C_0A_2 - A_0(C_0 - A_0)] \dots; \quad (\text{A15c})$$

$$a_0 = (2C_0)^{1/2}, \quad (\text{A16a})$$

$$a_2/a_0 = (4C)^{-1} (C_2 - 2C_0E_2) \dots; \quad (\text{A16b})$$

$$Q_1 = a_0E_2, \quad (\text{A17a})$$

$$Q_3 = 2a_0E_4 + a_2E_2, \dots \quad (\text{A17b})$$

The relations between the coefficients  $A$ ,  $C$ , and  $E$  as required by equations (44), (49a), and (49b) can be introduced to give the functional dependence of the above coefficients on the initial eccentricity  $e_0$ . This step is carried out later. The results for some of the more important coefficients are

$$E_0 = 1, \quad E_2 = \frac{1}{2} \left( 3 - \frac{4\pi}{c_0} \right); \quad (\text{A18a})$$

$$\frac{E_4}{E_2} = (6c_0^2)^{-1} \left( 2\pi \frac{c_1}{\epsilon_1} - \frac{a_0c_0}{\epsilon_1} \right); \quad (\text{A18b})$$

$$a_0 = (2c_0)^{1/2}, \quad \frac{a_2}{a_0} = (4c_0^2)^{-1} (c_0 - a_0) \left( \frac{c_1}{\epsilon_1} - 2c_0 \right); \quad (\text{A18c})$$

$$Q_1 = a_0E_2, \quad \frac{Q_3}{Q_1} = \frac{2c_4}{c_2} + \frac{a_2}{a_0}; \quad (\text{A18d})$$

where

$$a_0 = 2\pi - \frac{c_0}{2}, \quad c_0 = 4\pi \frac{1 - e_0^2}{e_0^2} \left( -1 + \frac{1}{2e_0} \log \frac{1 + e_0}{1 - e_0} \right), \tag{A18e}$$

$$c_1 = \frac{4\pi}{e_0^2} \left[ 3 - (3 - e_0^2) \frac{1}{2e_0} \log \frac{1 + e_0}{1 - e_0} \right], \quad \epsilon_1 = -\frac{e_0}{1 - e_0^2}. \tag{A18f}$$

TABLE A2

NUMERICAL VALUES FOR CERTAIN IMPORTANT COEFFICIENTS IN PROLATE CASE

$\omega_0/z_0$	$E_2$	$E_4/E_2$	$a_0$	$a_2/a_0$	$Q_1$	$Q_3/Q_1$
1 00	0	$+\infty$	2 895	0	0	$+\infty$
0 95	- 0 0637	0 726	2 83	0 0188	- 0 181	1 47
0 90	- 0 136	0 582	2 77	0 0392	- 0 376	1 20
0 80	- 0 312	0 502	2 63	0 0863	- 0 821	1 09
0 70	- 0 548	0 500	2 48	0 144	- 1 36	1 14
0 60	- 0 881	0 541	2 30	0 218	- 2 02	1 30
0 50	- 1 38	0 633	2 09	0 318	- 2 88	1 58
0 40	- 2 20	0 810	1 84	0 461	- 4 05	2 08
0 30	- 3 74	1 18	1 55	0 693	- 5 79	3 04
0 20	- 7 46	2 12	1 18	1 16	- 8 83	5 39
0 10	- 23 1	6 34	0 714	2 71	- 16 5	15 4
0 05	- 72 6	20 2	0 412	6 60	- 29 9	47 1
0 00	$-\infty$	$+\infty$	0	$+\infty$	$-\infty$	$+\infty$

Numerical values for the coefficients  $E_2$ ,  $E_4/E_2$ ,  $a_0$ ,  $a_2/a_0$ ,  $Q_1$ , and  $Q_3/Q_1$  are given in Table A2. The final formulae used for numerical computations are

$$E = 1 + E_2(\tan \theta)^2 + E_4(\tan \theta)^4, \tag{A19a}$$

$$Z = \cos^2 \theta, \tag{A19b}$$

$$R = EZ, \tag{A19c}$$

$$a_0 \tau = \theta + \frac{1}{2} \sin 2\theta - \frac{a_2}{a_0} \left( \theta - \frac{1}{2} \sin 2\theta \right). \tag{A19d}$$

*Expansion in (e - e<sub>0</sub>)*

To relate  $A$ ,  $C$ , and  $E$ , we expand them in powers of

$$\delta = e - e_0. \tag{A20}$$

We have

$$A = a_0 + a_1\delta + a_2\delta^2 + \dots, \tag{A21a}$$

$$C = c_0 + c_1\delta + c_2\delta^2 + \dots, \tag{A21b}$$

$$E = \epsilon_0 + \epsilon_1\delta + \epsilon_2\delta^2 + \dots. \tag{A21c}$$

It is clear that the coefficients above are functions only of  $e_0$  and can be obtained from the expressions (44), (49a), and (49b). Indeed some of these are given explicitly by equations (A18e) and (A18f). Since  $A$ ,  $C$ , and  $E$  are given in  $x$ , it is clear that  $\delta$  must be even in  $x$  and vanishes at  $x = 0$ ; thus

$$\delta = \delta_2 x^2 + \delta_4 x^4 + \dots \tag{A22}$$



Upon substitution of equation (A22) into equation (A21) and comparison with equations (53)–(55), we get

$$A_0 = a_0, \quad A_2 = a_1\delta_2, \quad A_4 = a_1\delta_4 + a_2\delta_2^2, \dots, \quad (\text{A23a})$$

$$C_0 = c_0, \quad C_2 = c_1\delta_2, \quad C_4 = c_1\delta_4 + c_2\delta_2^2, \dots, \quad (\text{A23b})$$

$$E_0 = \epsilon_0 = 1, \quad E_2 = \epsilon_1\delta_2, \quad E_4 = \epsilon_1\delta_4 + \epsilon_2\delta_2^2, \dots \quad (\text{A23c})$$

The coefficients in equations (A15)–(A17) can be obtained explicitly in terms of  $a_0, a_1, \dots; b_0, b_1, \dots; c_0, c_1, \dots$ , which are known functions of the initial eccentricity, by using equations (A23) in alternate steps with equations (A15)–(A17). Thus, the first equations of (A23a) and (A23b) coupled with equation (A15b) determine  $E_2$ . The second relation of (A23c) serves to define  $\delta_2$  once  $E_2$  is determined, from which  $A_2$  and  $C_2$  are obtained from the second equations of (A23a) and (A23b). This enables the calculation of  $E_4$  from equation (A15c). Partial results are summarized in equations (A18).

One of us (L. M.) wishes to thank Professor C. C. Lin for arranging a visit to the Department of Mathematics, Massachusetts Institute of Technology as research associate during July and August, 1964. The cosmogonical importance of the present problem first arose during discussions with Professor E. E. Salpeter during his visit to Cambridge, England, in 1961. The authors are grateful to the Computation Center at Massachusetts Institute of Technology for the use of its facilities.

This work is supported in part by the National Aeronautics and Space Administration through the Center for Space Research at Massachusetts Institute of Technology.

#### REFERENCES

- Chandrasekhar, S., and Fermi, E. 1953, *Ap. J.*, **118**, 113.  
 Gill, S. 1953, *Proc. Cambridge Phil. Soc.*, **47**, 96.  
 Hoyle, F. 1953, *Ap. J.*, **118**, 513.  
 Hunter, C. 1962, *Ap. J.*, **136**, 594.  
 ———. 1964, *ibid.*, **139**, 570.  
 Layzer, D. 1963, *Ap. J.*, **137**, 351.  
 Ledoux, P. 1951, *Ann. d'ap.*, **14**, 438.  
 Lynden-Bell, D. 1962, *Proc. Cambridge Phil Soc.*, **58**, 709.  
 ———. 1964, *Ap. J.*, **139**, 1195.  
 Lyttleton, R. A. 1953, *The Stability of Rotating Liquid Masses* (Cambridge: Cambridge University Press).  
 McCrea, W. H. 1957, *M.N.*, **117**, 562.  
 McMillan, W. D. 1958, *The Theory of the Potential* (New York: Dover Publications).  
 Mestel, L. 1965, *Q.J.R.A.S.* (in press).  
 Spitzer, L., Jr. 1942, *Ap. J.*, **95**, 329.  
 Strittmatter, P. A. 1965, *M.N.* (in preparation).